

# Excited States in $N^{14}$ from $C^{12}(d,d)C^{12}$ , $C^{12}(d,p_0)C^{13}$ , and $C^{12}(d,p_1)C^{13*}\dagger$

E. KASHY,\* R. R. PERRY, AND J. R. RISSE

*The Rice Institute, Houston, Texas*

(Received August 3, 1959)

Excited states in the  $N^{14}$  nucleus have been observed by measuring the differential scattering and reaction cross sections of  $C^{12}(d,d)C^{12}$ ,  $C^{12}(d,p_0)C^{13}$ , and  $C^{12}(d,p_1)C^{13*}$  for deuteron bombarding energies from 0.5 to 2.0 Mev. Resonances were investigated at deuteron bombarding energies of 0.92, 1.19, 1.31, 1.446, and 1.79 Mev, corresponding to excited states at 11.05, 11.29, 11.39, 11.503, and 11.80 Mev in  $N^{14}$ . Scattering matrix analysis of the elastically scattered deuterons and of angular distributions of the reaction protons to the ground state of  $C^{13}$  gave assignments of  $1^+$ ,  $2^-$ ,  $1^+$ ,  $3^+$ , and  $1^+$  for these states. The analysis of the  $C^{12}(d,p_0)C^{13}$  angular distributions at 0.92, 1.19, and 1.31 Mev indicated a reaction mechanism in which the relative proton-neutron spin orientation of the deuteron is preserved.

## INTRODUCTION

THE work reported here was part of an experimental investigation of states in  $N^{14*}$  between 8- and 12-Mev excitation formed by 0.5- to 5-Mev protons on  $C^{13}$  and/or 0.5- to 2-Mev deuterons on  $C^{12}$ .<sup>1</sup> There is considerable interest in the energy level scheme of  $N^{14*}$ .<sup>2</sup> Both experiments and analyses proved somewhat simpler in the case of deuterons on  $C^{12}$ , and this paper is concerned only with those  $N^{14*}$  states between 11- and 12-Mev excitation reached by 0.5- to 2-Mev deuterons. These states, while showing interference, were sufficiently well separated that analysis was feasible.  $C^{12}(d,d)C^{12}$ ,  $C^{12}(d,p_0)C^{13}$ , and  $C^{12}(d,p_1)C^{13*}$  excitation curves and  $C^{12}(d,p_0)C^{13}$  angular distributions were taken and analysis using a dispersion theory form of the scattering matrix was carried out. Since analysis involving a spin of unity is complicated by the fact that states of one parity, in this case  $(-)^{J-1}$ , can be formed by two values of orbital angular momentum, the necessary simplifications and their effect are discussed at some length in the body of the paper. The three states of lower energy, 11.05, 11.29, and 11.39 corresponding to resonances at 0.92, 1.19, and 1.31 Mev, were found to decay to the ground state of  $C^{13}$  predominantly by channel spin zero. To the extent that the  $C^{13}$  ground state consists of a single particle neutron state with  $l_n=1$  and  $J^\pi=1/2^-$ , the channel-spin-zero decay mode means that the protons are emitted from a triplet spin state, as though the relative neutron-proton spin orientation of the deuteron were preserved throughout the reaction. It is probable that these states are  $T=0$  states. Isotopic spin selection rules allow excitation only of  $T=0$  states in  $N^{14*}$  by deuterons on  $C^{12}$ . There is interest in the question of isotopic spin conservation in heavy particle reactions which proceed by

way of highly excited states, such as those involved here.<sup>3</sup>

In addition to elastic scattering, three reactions of importance occur when  $C^{12}$  is bombarded by 0.5- to 2-Mev deuterons:  $C^{12}(d,p_0)C^{13}$  ( $Q=2.73$ );  $C^{12}(d,p_1)C^{13*}$  ( $Q=-0.37$ ); and  $C^{12}(d,n_0)N^{13}$  ( $Q=-0.28$ ). While no previously published work has been found on the elastic scattering of deuterons below 2 Mev, there have been many experiments on the reactions. The original  $C^{12}(d,n)N^{13}$  investigation was done by Bennett and Bonner.<sup>4</sup> Since then a number of more recent papers on the same reaction has been published including that of Bonner, Evans, Harris, and Phillips,<sup>5</sup> who gave a number of angular distributions of the neutrons in the range of deuteron bombarding energies from 0.7 to 2 Mev. These were used in the present paper for calculating neutron partial widths. Values for the absolute cross section at  $0^\circ$  are found in curves of charged particle cross sections compiled by Jarmie and Seagrave.<sup>6</sup> The  $(d,p_0)$  reaction in the 0.5- to 2-Mev energy range has been investigated by Phillips,<sup>7</sup> who obtained a number of angular distribution and three excitation curves of the long-range protons. This reaction was also investigated by Sarma, Govindjee, and Allan<sup>8</sup> whose work closely parallels that of Phillips.<sup>7</sup> However, there are large discrepancies between the absolute values of the differential cross sections given in these two papers. The protons to the 3.09-Mev state of  $C^{13}$  from the reaction  $C^{12}(d,p_1)C^{13*}$  have not previously been studied, except in reference 8 where they were observed in the immediate neighborhood of the 1.446-Mev resonance. The 3.09-Mev  $\gamma$  rays associated with these protons were observed in reference 5.

<sup>3</sup> E. P. Wigner, Proceedings of Robert A. Welch Foundation Conferences on Chemical Research, Houston, Texas, 1957, (unpublished), Vol. 1, p. 67.

<sup>4</sup> W. E. Bennett and T. W. Bonner, Phys. Rev. **58**, 183 (1940).

<sup>5</sup> Bonner, Evans, Harris, and Phillips, Phys. Rev. **75**, 1401 (1949).

<sup>6</sup> N. Jarmie and J. D. Seagrave, Los Alamos Scientific Laboratory Report LA-2014 (unpublished).

<sup>7</sup> G. C. Phillips, Phys. Rev. **80**, 164 (1950).

<sup>8</sup> Sarma, Govindjee, and Allan, Proc. Phys. Soc. (London) **A70**, 68 (1957).

<sup>†</sup> Supported in part by the U. S. Atomic Energy Commission.

\* Now a National Science Foundation Postdoctoral Fellow at Massachusetts Institute of Technology, Cambridge, Massachusetts.

<sup>1</sup> Kashy, Perry, and Risser, Bull. Am. Phys. Soc. **4**, 96 (1959).

<sup>2</sup> Warburton, Rose, and Hatch, Phys. Rev. **114**, 214 (1959), and and references listed in that paper.

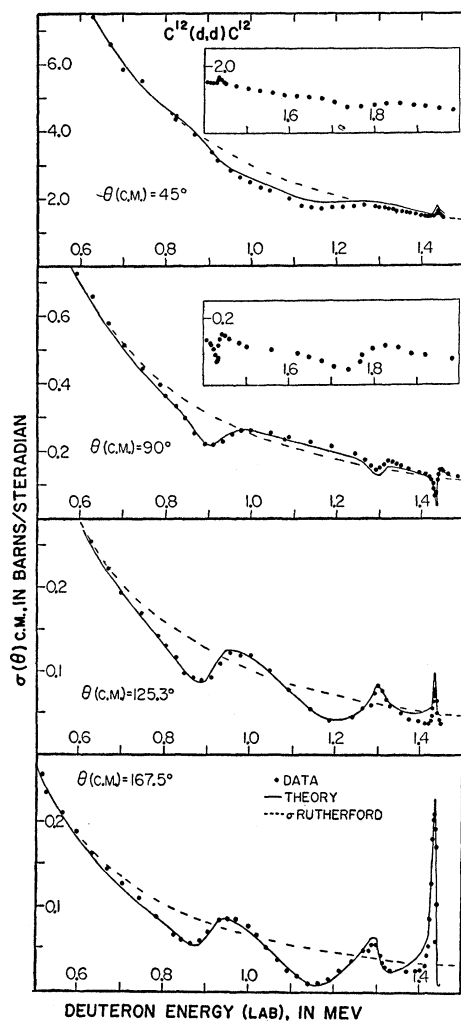


FIG. 1. Center-of-mass differential cross section for the scattering of deuterons by  $C^{12}$ . The solid lines represent the theoretical fits.

#### EXPERIMENTAL PROCEDURE

The scattering chamber was designed for the use of thin self-supporting foils as targets.<sup>9</sup> The chamber consisted mainly of two shallow cylinders. The lower remained fixed, while the upper could be rotated with respect to the lower. The target was mounted in the lower cylinder, which also contained the beam defining slits. The detector and the slit system defining the solid angle for scattering into the detector were mounted in the upper cylinder at  $75^\circ$  to its axis of rotation. The angle of scattering was set in terms of the angle  $\phi$ , indicated by graduations which were made on the top and bottom halves of the chamber. The angle of scattering  $\theta$  is then  $\arccos(\cos 15^\circ \cos \phi)$ . The over-all accuracy of the angle of scattering was estimated to be  $\pm 0.5^\circ$ .

The Rice Institute 5.5-Mev Van de Graaff accelerator

<sup>9</sup> Kashy, Perry, and Risser, *Nuclear Instr. and Methods* **4**, 167 (1959).

was used to accelerate the deuterons. The integration of the incident beam was done in a Faraday cup with an electron suppressing voltage of 300 volts applied to a ring in the front of the Faraday cup. The carbon targets used in these reactions consisted of  $C^{12}$  foils of about  $20 \mu\text{g}/\text{cm}^2$  which were self-supporting over a circular area of approximately 0.8 cm in diameter. The method of preparation of the foils is described elsewhere.<sup>9</sup> One foil whose thickness was about 5 kev at 1.4-Mev deuteron bombarding energy was used for most of the experiment. The energy of the incident beam was determined using a  $90^\circ$  analyzing magnet which was calibrated in terms of the frequency of a proton-moment detector, taking the  $\text{Li}^7(p,n)\text{Be}^7$  and  $C^{13}(p,n)\text{N}^{13}$  neutron thresholds as the calibration energies. The detection of the scattered particles was done using a scintillation counter consisting of a 0.025-inch thick  $\text{CsI(Th)}$  crystal mounted on a DuMont-6291 photomultiplier tube.

In order to obtain absolute values of the differential cross section in both the  $(d,d)$  and the  $(d,p)$  channels, we have normalized the elastically scattered deuteron yield to the Rutherford cross section for deuterons at 0.5 Mev. This normalization was checked in terms of the published differential cross section<sup>10</sup> for the scattering of protons by  $C^{12}$  at an incident proton energy of 3 Mev. Since the carbon foils used in this experiment were extremely thin, the cracking of carbohydrates from the vacuum system onto the foils resulted in a sizeable increase in the thickness of the target. At the end of an extended run on an excitation curve or angular distribution, a correction for this effect was obtained by taking a number of widely spaced check points in quick succession. During all of the experiment with the very thin foils, the beam was kept off the target between data points.

The reaction protons from  $C^{12}(d,p_0)C^{13}$  and  $C^{12}(d,p_1)C^{13*}$  were measured simultaneously with, and consequently under the same experimental conditions of solid angle, target thickness, etc., as the elastically scattered deuterons. The proton reaction cross sections were thus determined directly in terms of the deuteron elastic cross section. Considering errors in charge integration, solid angle and the determination of target thickness, but excluding statistical errors of counting which in general were less than 3%, the uncertainties in the elastic cross sections are estimated to be less than  $\pm 6\%$  and the uncertainties in the  $(d,p)$  cross sections to be less than  $\pm 8\%$ . The angular distributions of the ground-state protons were taken with a thin nickel foil in front of the  $\text{CsI}$  crystal in order to prevent the flooding of the detector with pulses at forward angles where  $\csc^4(\theta/2)$  was large. The foil was thick enough to stop the elastically scattered deuterons while thin enough to allow the protons to penetrate easily to the crystal.

<sup>10</sup> Reich, Phillips, and Russell, *Phys. Rev.* **104**, 143 (1956).

C<sup>12</sup>(d,d)C<sup>12</sup>

## a. Experimental Results

We have taken excitation curves of the elastically scattered deuterons at center-of-mass angles 45°, 54.7°, and 90° for deuteron energies from 0.5 to 2 Mev and at center-of-mass angles 125.3° and 167.5° for energies from 0.5 to 1.5 Mev. Except for the 54.7° curve which was similar to the one at 45°, these data are plotted in Fig. 1. Anomalies in the differential cross section can be attributed to resonances at deuteron bombarding energies of 0.92, 1.19, 1.31, 1.446, and 1.79 Mev.

The 125.3° and 167.5° curves were terminated at 1.5 Mev because the deuteron pulses could not be satisfactorily resolved from the first-excited-state-proton pulses above 1.5 Mev. Above 1.25 Mev at these angles, resolution was not complete, and errors in the elastic data may be somewhat greater than the ±6% quoted for the data as a whole.

## b. Analysis

Since the levels under investigation were broad, it was clearly necessary in the analysis to include a

TABLE I. Allowed values of the orbital angular momentum for indicates channel spins.

$J\pi$	$l_d$ $S=1$	$l_{p0}$ (or $l_{n0}$ ) $S'=0$ $S'=1$	$l_{p1}$ $S'=0$ $S'=1$
0 <sup>-</sup>	1	0	...
0 <sup>+</sup>	...	...	1
1 <sup>-</sup>	1	...	1
1 <sup>+</sup>	0, 2	1	...
2 <sup>-</sup>	1, 3	2	...
2 <sup>+</sup>	2	...	2
3 <sup>-</sup>	3	...	3
3 <sup>+</sup>	2, 4	3	...
4 <sup>-</sup>	3, 5	4	...
4 <sup>+</sup>	4	...	4

number of states with interference between them. A form for the differential cross section was used in which the amplitudes of the scattered partial waves were expressed in terms of the incident partial wave amplitudes by a scattering matrix from the single level approximation of dispersion theory:

$$\frac{d\sigma}{d\Omega} = \sum_{s,m_s} \frac{1}{(2I+1)(2i+1)} |f_s^{m_s}(\theta, \varphi)|^2, \quad (1)$$

where  $S$  is the channel spin index, and<sup>11</sup>

$$k f_s^{m_s}(\theta, \varphi) = -(\eta/2) \csc^2(\theta/2) \exp[i\eta \ln \csc^2(\theta/2)] \chi_s^{m_s} \\ + \sum_{J, m_s', l, l'} [\pi(2l'+1)]^{1/2} i^{l'-l+1} Y_l^{m_s-m_s'}(\theta, \varphi) \\ \times \chi_s^{m_s'}(l s m_s - m_s' m_s' | l s J m_s) \\ \times (l' s 0 m_s | l' s J m_s) (e^{2i\alpha l} \delta_{ll'} - S_{ll'}^J e^{-2i\sigma_0}),$$

<sup>11</sup> C. W. Reich, Ph.D. thesis, The Rice Institute, 1956 (unpublished).

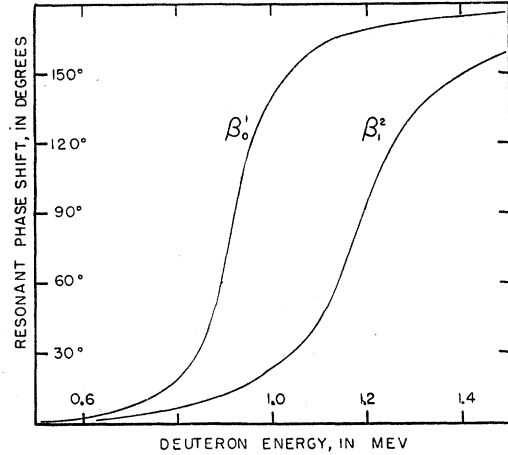


Fig. 2. Resonant phase shift  $\beta^{J\pi}$  used for the 0.92- and 1.19-Mev resonances.

with

$$S_{ll'}^J e^{-2i\sigma_0} = e^{i(\alpha l + \alpha l' + \varphi l + \varphi l')} \\ \times \left\{ \delta_{ll'} + \frac{(\Gamma_l)^{1/2} (\Gamma_{l'})^{1/2}}{\Gamma} [\exp(2i\beta^{J\pi}) - 1] \right\}, \\ \beta^{J\pi} = \arctan[\Gamma/2(E_0 - E)].$$

The symbols are defined in Appendix A. To obtain the real and imaginary parts of  $f_s^{m_s}(\theta, \varphi)$ , numerical values of the Wigner coefficients were calculated from their form.<sup>12</sup> Some of the complexities of the  $S=1$  scattering problem have been discussed elsewhere.<sup>13,14</sup> The single level dispersion theory approximation appears justified by the success obtained in making the assignments. The states of parity  $(-)^{J-1}$ , except  $J=0$  states, can be made with two values of  $l_d$ .  $l_d$  can change during scattering from these states. However, in all but one of the cases a single value of  $l_d$  was sufficient to explain the elastic data. As discussed later, a small mixing of  $l_d$  values was necessary in the case of the 1.31-Mev resonance.

In programming expression (1) for the IBM-650 computer, entries for the parameters of ten resonances were included, so that the effect of states with all angular momentum and parity values from 0<sup>-</sup> to 4<sup>+</sup> could be taken into account. After inserting the widths, the behavior of the resonances was obtained from the variations of the  $\beta^{J\pi}$ . For the broad low-energy 0.92- and 1.19-Mev resonances, where penetrabilities changed markedly over the resonances, instead of  $\tan^{-1}[\Gamma/2(E_0 - F)]$ , the dependence of  $\beta^{J\pi}$  shown in Fig. 2 was used.

All possible  $l$  values for given  $J$  and  $\pi$  are shown in Table I. In order to reduce the number of starting combinations of  $J$ ,  $\pi$ , and  $l_d$  to be used in computing

<sup>12</sup> J. M. Blatt and V. F. Weisskopf, *Theoretical Nuclear Physics* (John Wiley and Sons, Inc., New York, 1952), p. 792.

<sup>13</sup> Kashy, Miller, and Risser, *Phys. Rev.* **112**, 547 (1958).

<sup>14</sup> J. M. Blatt and L. C. Biedenharn, *Phys. Rev.* **86**, 399 (1952).

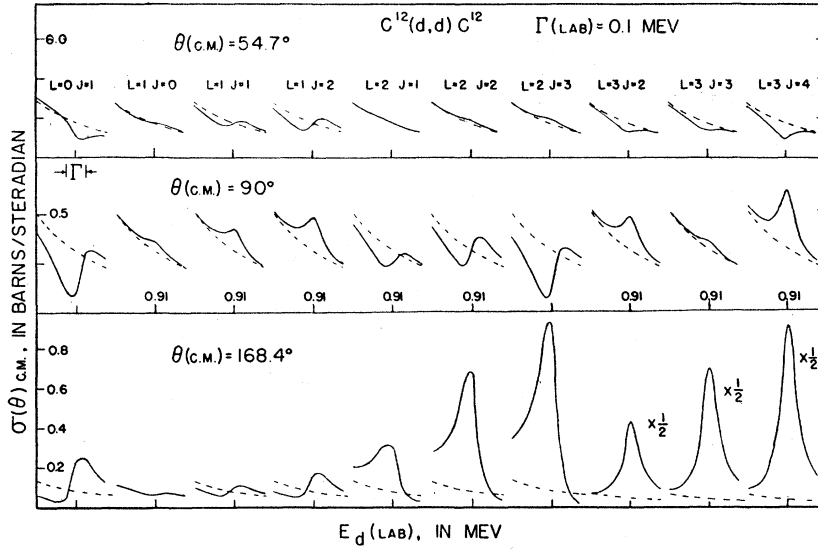


FIG. 3. Theoretical isolated resonance curves for the elastic scattering of deuterons by  $C^{12}$ . The resonant energy is 0.9 Mev and the width is 100 kev.

fits to the experimental data, isolated single-level resonance curves for the differential cross section for all possible  $J$ ,  $\pi$ , and  $l_d$  values were computed at several energies. By comparison between observed and calculated resonance shapes, the possible assignments for each of the lowest five resonances could be restricted to at most two combinations of  $J$ ,  $\pi$ , and  $l_d$ . Computations were then carried out for these starting possibilities. After having determined  $J$  and  $\pi$  for each state, relative widths  $\Gamma_d/\Gamma$  were varied until best agreement was obtained between data and theory.

The solid lines of Fig. 1 represent the best fit obtained to the elastic data. The assignments were the final assignments, taking into account the analysis of the  $C^{12}(d, p_0)C^{13}$  angular distributions and the character of the  $C^{12}(d, n_0)N^{13}$  angular distributions. The assignments and widths are found in Table II.

The discussions of the assignments are found under results.

A typical set of  $C^{12}(d, d)C^{12}$  single level resonance curves from isolated states is shown in Fig. 3 for center-of-mass angles  $54.7^\circ$ ,  $90^\circ$ , and  $168.4^\circ$ . All allowed combinations  $l_d$ ,  $J$ , and  $\pi$  are shown without  $l$  mixing for  $l_d \leq 3$  using  $E_0 = 0.9$  Mev and  $\Gamma = 100$  kev. These curves are included because they exhibit typical resonance behavior of elastically scattered charged particles with unit channel spin. It is easily seen by inspection of Figs. 1 and 3 that, for example, the anomaly at

0.9 Mev in the experimental data can be due only to a  $J^\pi = 1^+$  ( $l_d = 0$ ) state.

### $C^{12}(d, p_0)C^{13}$

#### a. Experimental Results

Four excitation curves of the ground-state protons were taken at laboratory angles of  $47.6^\circ$ ,  $80.5^\circ$ ,  $158.4^\circ$ , and  $165.0^\circ$ . These curves are shown in Fig. 4. Resonance phenomena were observed at deuteron bombarding energy of 0.92, 1.19, 1.31, and 1.446 Mev, and the behavior of the data between 1.6 and 1.9 Mev indicated at least two additional resonances whose position and width were uncertain. Angular distributions were measured for deuteron bombarding energies of 0.92, 1.19, 1.31, 1.62, and 1.76 Mev, i.e., on resonance. Data were obtained for at least sixteen angles on each distribution. The conversion of these angular distributions from the laboratory to the center-of-mass system was done using the tables by Marion,<sup>15</sup> using 2.73 Mev for the  $Q$  value. The reduced angular distribution data in center-of-mass coordinates are shown in Figs. 5 and 6. The agreement of the present work with that of Phillips,<sup>7</sup> and Sarma *et al.*<sup>8</sup> is good except for the discrepancy in the absolute value of the differential cross section.

#### b. Analysis

The analysis of angular distributions from  $C^{12}(d, p_0)C^{13}$  played an essential part in the assignments of the states, since the angular distribution of the protons made it possible to resolve ambiguities in  $J$  and  $\pi$  which remained after the analysis of the elastically scattered deuterons. An example was the 1.19-Mev state which could have been mistaken for a  $1^-$  state from the

TABLE II. Angular momenta, parities, and laboratory widths of the states of  $N^{14}$ .

$E$ $N^{14}$ (Mev)	$E_d$ (lab)	$l_d$	$J^\pi$	$\Gamma_d$ (kev)	$\Gamma_p$ (kev)	$\Gamma_{p1}$ (kev)	$\Gamma_n$ (kev)	$\Sigma \Gamma$ 's (kev)	$\Gamma_{exp}$ (kev)
11.05	0.92	0	$1^+$	29	44	22	22	$117 \pm 15$	110
11.29	1.19	1	$2^-$	79	154	11	31	$275 \pm 35$	220
11.39	1.31	2, (0)	$1^+$	15	9	5	4	$33 \pm 6$	35
11.503	1.446	2	$3^+$	4	1	1	1	$6 \pm 1$	6
11.80	1.79	0	$1^+$	50	...	...	...	...	100

<sup>15</sup> J. B. Marion, Atomic Energy Commission Report NP-6241 (unpublished).

elastically scattered deuteron data alone. Least squares fits to the experimental angular distribution data were obtained and proved a great help in arriving at the final assignments. Probable sets of parameters were entered in an IBM-650 program and varied until best

fit was obtained with the experimental data. The analysis was based on Eqs. (3.16), (4.5), and (4.6) of Blatt and Biedenharn<sup>16</sup> which were derived on the basis of single level dispersion theory. The expression actually programmed was

$$\frac{d\sigma}{d\Omega} = \sum_{ss'L} \frac{(-1)^{s'-s}}{k^2(2i+1)(2I+1)} \sum_{J_1 J_2 l_1 l_2 l_1' l_2'} Z(l_1 J_1 l_2 J_2; sL) Z(l_1' J_1 l_2' J_2; s'L) P_L(\cos\theta) \times \frac{\cos(\sigma_{l1} + \varphi_{l1} + \sigma_{l1'} + \varphi_{l1'} + \beta_1 - \sigma_{l2} - \varphi_{l2} - \sigma_{l2'} - \varphi_{l2'} - \beta_2)(\Gamma_{l1})^{\frac{1}{2}}(\Gamma_{l1'})^{\frac{1}{2}}(\Gamma_{l2})^{\frac{1}{2}}(\Gamma_{l2'})^{\frac{1}{2}}}{\{[(E_1 - E)/\frac{1}{2}\Gamma_1]^2 + 1\}^{\frac{1}{2}}\{[(E_2 - E)/\frac{1}{2}\Gamma_2]^2 + 1\}^{\frac{1}{2}}\Gamma_1\Gamma_2}. \quad (2)$$

The symbols are defined in Appendix A. The  $Z$  coefficients are numerically tabulated in several places.<sup>17,18</sup> Possible contributions from direct interaction processes were not considered.

Since the  $Q$  value is large and positive in the case of  $C^{12}(d, p_0)C^{13}$ , the penetrability argument for neglecting the higher value of the orbital angular momentum of the reaction particle is generally not valid, even though the difference in orbital angular momentum value must be 2. However, as will be seen later, the angular distributions were found to correspond to excited states which decay predominantly through one  $l_p$  value.

In the  $C^{12}(d, p_0)C^{13}$  reaction,  $S=1$  and  $S'=0$  or 1. As indicated in Table I, states of parity  $(-)^{J-1}$ , except states with  $J=0$ , can decay by either channel spin. For  $0^-$  states,  $S'=0$ . For the remaining states,  $S'$  can only be 1. Because of the square root in the expression for the cross section there is an ambiguity as to the sign of the interference term, so that the sum for two resonances is of the form  $J_1 J_1 + J_2 J_2 \pm A J_1 J_2$ , where  $A \leq 2$ . The sign ambiguity was usually easily resolved from the experimental data. The magnitude of the cross section is determined by the value of the product of the relative widths  $\Gamma_d \Gamma_p / \Gamma^2$  in the incident and reaction channels, since the angular distributions were taken at the resonance energies. The absolute cross section values thus determined the proton partial widths. Individual fits are discussed in the results.

### $C^{12}(d, p_1)C^{13*}$

One excitation curve of the protons to the first excited state of  $C^{13}$  was taken at a laboratory angle of  $80.5^\circ$  and is shown in Fig. 7. Since  $80.5^\circ$  is a good approximation to  $90^\circ$  c.m. over the whole energy range, and since odd interference terms are zero at  $90^\circ$  c.m., these data were used in calculating partial and reduced widths for  $p_1$  emission. Consideration was also given to previously published  $C^{12}(d, p_1\gamma)C^{13*}$  data<sup>5</sup> in the estimates of the partial width.

<sup>16</sup> J. M. Blatt and L. C. Biedenharn, Revs. Modern Phys. **24**, 258 (1952).

<sup>17</sup> L. C. Biedenharn, Oak Ridge National Laboratory Report ORNL-1501 (unpublished).

<sup>18</sup> Sharp, Kennedy, Sears, and Hoyle, Atomic Energy of Canada Limited Report, AECL-97 (unpublished).

### $C^{12}(d, n_0)N^{13}$

In calculating the neutron partial widths found in Table II, the angular distributions of Bonner *et al.*<sup>5</sup>

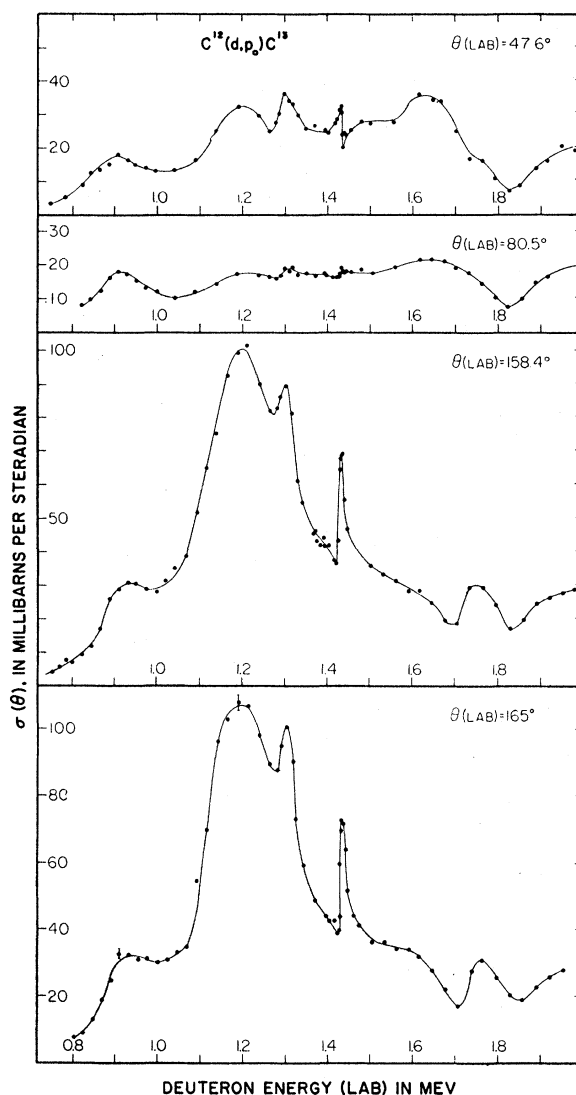


FIG. 4. Laboratory differential cross section for the  $C^{12}(d, p_0)C^{13}$  reaction.

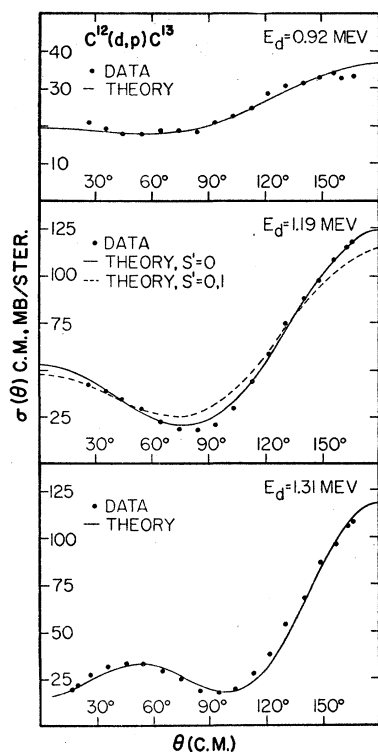


FIG. 5. Angular distribution of the ground-state protons at 0.92, 1.19, and 1.31 Mev.

were integrated numerically to obtain the total cross section in terms of the differential cross section at  $0^\circ$ , and the  $0^\circ$  values of the cross section were taken from the Los Alamos compilation.<sup>6</sup> In the integrations, no assumption was made as to mode of decay, and both  $S'=1$  and  $S'=0$  were used.

The neutron angular distributions are in qualitative

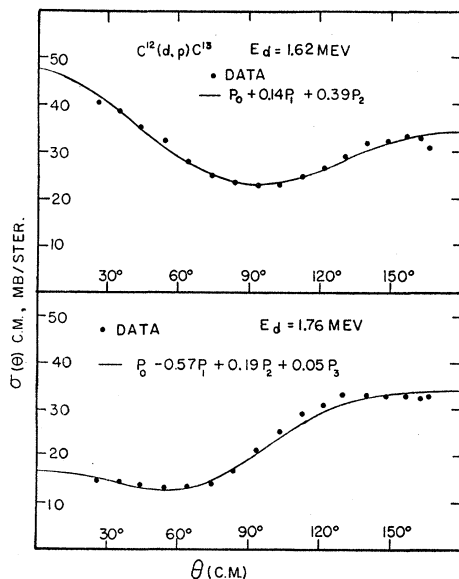


FIG. 6. Angular distributions of the  $C^{13}$  ground-state protons at 1.61 and 1.76 Mev.

agreement with the distributions to be expected from the states listed in Table II.

## RESULTS

### The 11.05-Mev State ( $E_d=0.92$ Mev):

$$J^\pi=1^+; l_d=0; S'=0; l_p=1$$

#### a. (d,d)

The assignment was obtained unambiguously from the analysis of the elastic deuteron data. No improvement in fit resulted from any admixture of  $l_d=2$ . Best fit was obtained from  $\Gamma_d/\Gamma=0.26$ . The fit is shown by the solid curves of Fig. 1.

#### b. (d,p<sub>0</sub>)

In the proton angular distribution there is a large amount of interference from a neighboring state of odd

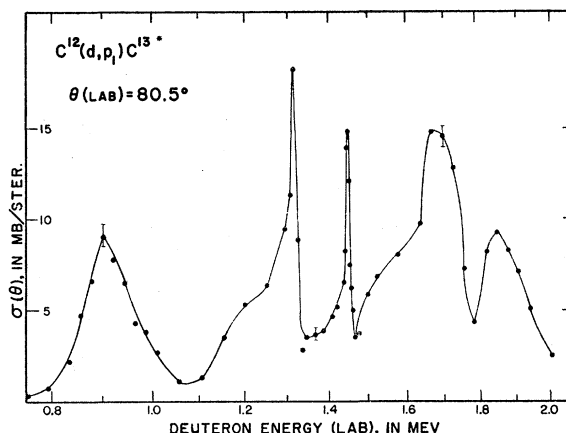


FIG. 7. Laboratory differential cross section for the  $C^{12}(d,p_1)C^{13}$  reaction. The protons are to the first excited state of  $C^{13}$ .

parity. The least squares fit was found to be

$$W(\theta) \sim P_0 - 0.36P_1 + 0.26P_2.$$

The calculated distribution from a  $J^\pi=1^-(l_d=0)$  state with interference from a  $2^-(l_d=1)$  state at 11.29 Mev is given by

$$\sigma(\theta) = 23(P_0 - 0.38P_1 + 0.23P_2) \text{ mb/sterad},$$

using a value of 0.1 for  $\Gamma_d\Gamma_p/\Gamma^2$ , and using widths for the 11.29-Mev state given in the next section. To obtain this expression,  $S'$  was taken equal to zero. If the contribution from  $S'=1$  had been added, the coefficient of  $P_1$  would have been decreased by a factor  $\frac{1}{2}$ . The calculated angular distribution is in good agreement with the experimental data, as shown in Fig. 5.

### The 11.29-Mev State ( $E_d=1.19$ Mev):

$$J^\pi=2^-; l_d=1; S'=0; l_p=2$$

#### a. (d,d)

The analysis of the elastic data could only restrict the assignment to  $1^-$  or  $2^-$ . The fit shown in Fig. 1 was

obtained with the  $2^-$  assignment, as required by the proton data, using  $\Gamma_d/\Gamma=0.36$ . No improvement was obtained from any admixture of  $l_d=3$ .

b.  $(d, p_0)$

The analysis of the proton data was necessary to take the ambiguity out of the assignment. A least squares fit for the  $(d, p_0)$  angular distribution gave

$$W(\theta) \sim P_0 - 0.75P_1 + 1.08P_2 - 0.03P_3.$$

For an isolated  $2^-$  level formed with  $l_d=1$ , the theoretical proton angular distributions are: using  $S'=0$  only,  $P_0+P_2$ ; using  $S'=1$  only,  $P_0+0.5P_2$ ; and using equal proton partial widths for decay into the  $S'=0$  and  $S'=1$  channels,  $P_0+0.75P_2$ . Comparison of the coefficients of  $P_2$  in these expressions with that in the least squares fit shows that the proton emission is almost entirely by channel spin zero, since the 0.92-Mev resonance does not contribute to the  $P_2$  coefficient while the contribution from the narrow 1.31-Mev resonance, which is of opposite parity, is negligible. Interference from the  $1^+$  state at 11.05 Mev ( $E_d=0.92$  Mev) is sufficient to explain the odd terms in the experimental distribution. Including this interference, the calculated distribution for  $S'=0$  is

$$\sigma(\theta) = 4.73(P_0 - 0.73P_1 + 0.98P_2 - 0.05P_3) \text{ mb/sterad}$$

using 0.23 for the quantity  $\Gamma_d\Gamma_p/\Gamma^2$  and using the parameters for the 11.05-Mev state quoted in the previous section. The solid curve of Fig. 5 is a plot of this expression. The fit is considerably better than it is for the dashed curve, which is a plot of the calculated distribution taking a combination of  $S'=0$  and  $S'=1$  with equal partial widths and also including interference from the 11.05-Mev state.

The assumption that proton decay can take place only with  $S'=0$  does not appear unreasonable in the light of a vector model. If we consider the ground state of C<sup>13</sup> to be a single particle state with  $l_n=1$  and with the neutron spin opposed to its orbital angular momentum, it is clear that  $S'=0$  represents the case in which the neutron and proton spins are parallel to each other and antiparallel to  $l_n$ , as though the relative neutron-proton spin orientation of the deuteron were preserved throughout the reaction. The implication of a single particle deuteron state is worthy of remark.

**The 11.39-Mev State ( $E_d=1.31$  Mev):**

$$J^\pi=1^+; l_d=2, (0); S'=0; l_p=1$$

a.  $(d, d)$

It was clear from comparison of the elastic deuteron data with the isolated resonance shapes of Fig. 3 that the orbital angular momentum value for this state was even and equal either to 0 or 2. From a number of calculations using  $l_d=0$ , the possibility of the state  $J^\pi=1^+(l_d=0)$  was ruled out since it gave results in

obvious contradiction with the observed cross section, and the fact that the state was formed mainly by  $l_d=2$  was definitely established. The limitation  $\Gamma_{d0}^2 \ll \Gamma_{d2}^2$ , with the possibility  $\Gamma_{d0}=0$ , seemed at first sight to restrict the  $J$  assignment to 2 or 3. Theoretical curves for a  $J^\pi=3^+(l_d=2)$  state clearly gave the wrong shape for the resonance, while large discrepancies remained between theory and experiment when  $J^\pi=2^+(l_d=2)$  was assumed. At this point the cross section was remeasured experimentally, and it was established that the discrepancy between data and theory was not due to error in the experimental data. Calculations were then carried out for a  $J^\pi=1^+(l_d=2)$  assignment. This is the assignment used in the fit plotted in Fig. 1. As can be seen, there is good agreement between data and theory. The fit was not sensitive to small admixtures of  $l_d=0$ , provided  $\Gamma_{d0}^2 \ll \Gamma_{d2}^2$ . From the fits obtained with admixtures of  $l_d=0$  we believe that an upper limit of 0.3 can be set for  $\Gamma_{d0}/\Gamma_{d2}$ .

b.  $(d, p_0)$

The least squares fit to the proton angular distribution taken on resonance was

$$W(\theta) \sim P_0 - 0.69P_1 + 0.94P_2 - 0.18P_3.$$

Interference from the opposite parity 11.29 Mev  $2^-(l_d=1)$  state was enough to explain the odd terms. The contributions to the  $P_0$  and  $P_2$  coefficients from the 1.19-Mev resonance were equal. This meant that the  $P_0$  and  $P_2$  contributions from the state itself must be approximately equal. An isolated  $J^\pi=1^+(l_d=2)$  state yields the following terms: using  $S'=0$  only,  $P_0+P_2$ ; using  $S'=1$  only,  $P_0-0.5P_2$ . This indicates that the decay of the state must take place with  $S'=0$ .

The theoretical angular distributions in the neighborhood of the resonance are sensitive to small admixtures of  $l_d=0$ . This sensitivity is due to the fact that for a  $J^\pi=1^+$  assignment the coefficient of  $P_1$  arises mainly from  $l_d=0$ , and the coefficient of  $P_3$  from  $l_d=2$ , in the interference with the  $2^-(l_d=1)$  state. The size of the  $P_1$  interference term in this distribution indicates the necessity of having  $l_d=0$  deuterons contributing to the formation of the state. The assignment of the state and the mixing of  $l$ 's in the incident channel are confirmed by the behavior of  $P_1$ ,  $P_3$ , and the  $P_3/P_1$  ratio in the neighborhood of the resonance. Experimental values of this ratio and of the coefficients of  $P_1$  and  $P_3$  obtained from data by Sarma *et al.*<sup>8</sup> are listed in Table III.

The final calculated angular distribution was found to be

$$\sigma(\theta) = 34(P_0 - 0.66P_1 + 0.90P_2 - 0.84P_3) \text{ mb/sterad},$$

using  $\Gamma_{d0}\Gamma_p/\Gamma^2=0.03$ ,  $\Gamma_{d2}\Gamma_p/\Gamma^2=0.11$ ,  $S'=0$ , and the parameters of the 11.29-Mev state quoted in the previous section. Comparison between theory and experiment are shown in Fig. 5 where the solid curve

TABLE III. Ratio of  $P_3$  coefficients to  $P_1$  coefficients in the  $C^{12}(d,p)C^{13}$  angular distributions.<sup>a</sup>

$E_d$ (Mev)	$P_1$	$P_3$	$P_3/P_1$
0.925	-0.33	-0.02	0.06
0.976	-0.38	0.06	-0.15
1.013	-0.56	0.12	-0.21
1.060	-0.70	-0.05	0.08
1.111	-0.54	0.08	-0.14
1.154	-0.73	-0.12	0.15
1.195	-0.64	0.05	-0.07
1.249	-0.75	-0.06	0.08
1.277	-0.76	-0.23	0.30
1.314	-0.48	-0.66	1.37
1.352	-0.31	-0.24	0.79
1.391	-0.21	-0.07	0.35
1.413	-0.05	0.13	-0.28
1.432	-0.69	-0.29	-0.42
1.458	-0.63	-0.27	-0.43
1.477	-0.28	-0.12	-0.43

<sup>a</sup> Calculated from data of Sarma, Govindjee, and Allan (reference 8).

is the final calculated distribution. Agreement is seen to be good.

**The 11.503-Mev State ( $E_d = 1.446$  Mev):**  
 $J = 3^+; l_d = 2$

The energy of this resonance was obtained from the calibration of the  $90^\circ$  analyzing magnet using the  $Li^7(p,n)Be^7$  and  $C^{13}(p,n)N^{13}$  threshold as calibration at 1.8811 and 3.236 Mev. The assignment of this state from the elastic data is unambiguous as  $J^\pi = 3^+, l_d = 2$ . The values of  $\Gamma_d/\Gamma$  used in fitting the data was 0.65 so that  $\Gamma_d = 4$  kev.

**The 11.80-Mev State ( $E_d = 1.79$  Mev):**  
 $J = 1^+; l_d = 0$

The elastically scattered deuterons at  $90^\circ$  in the center of mass indicate a resonance energy of 1.79 Mev and a  $J^\pi = 1^+(l_d = 0)$  assignment for this state. The width  $\Gamma_d/\Gamma \approx 0.5$ . There is also indication of interference from an  $l_d = 1$  resonance. It was not possible to determine either the resonant energy or  $J^\pi$  of the state causing the interference.

Two angular distributions of the ground-state protons were taken with the following results: at 1.61 Mev the least squares fit to the angular distribution was of the form

$$W(\theta) \sim P_0 - 0.14P_1 + 0.39P_2,$$

while the 1.76-Mev angular distribution was

$$W(\theta) \sim P_0 - 0.57P_1 + 0.19P_2 + 0.05P_3.$$

The expressions are plotted as the solid curves in Fig. 6.

The 1.61-Mev distribution is almost symmetric about  $90^\circ$  while the 1.76-Mev distribution is quite asymmetric. This is additional evidence that there must be two states of opposite parity in this energy region. The anomalies in the excitation curves of the  $C^{12}(d,p_0)C^{13}$  reaction are in qualitative agreement with the existence of the 11.80-Mev state with  $J^\pi = 1^+(l_d = 0)$  ( $E_d = 1.79$ ) and give additional evidence for a resonance in the 1.6 and 1.7-Mev region due to a negative parity state.

### PARTIAL AND REDUCED WIDTHS

In Table II, the energy widths, and assignments of the levels are tabulated together with the partial widths for emission in the various possible channels. Finally, in Table IV, we have listed the reduced widths

TABLE IV. Reduced widths.

$E$ N <sup>14</sup> *	$\gamma_{d^2}$	%	$\gamma_{p^2}$	%	$\gamma_{p^1}$	%	$\gamma_{n^2}$	%
(Mev)	(Mev)	W.L.	(Mev)	W.L.	(Mev)	W.L.	(Mev)	W.L.
11.05	0.093	7%	0.022	0.8%	0.44	14%	0.07	2%
11.29	0.268	19%	0.192	6.2%	0.30	10%	0.5	16%
11.39	0.250	18%	0.004	0.1%	0.02	0.7%	0.005	0.2%
11.503	0.043	3%	0.005	0.2%	0.14	5%	...	...
11.80	0.032	2%	...	...	...	...	...	...

and percentages of the Wigner limit for each resonance for the various possible channels.

### ACKNOWLEDGMENT

We are very grateful to the Shell Development Company for the generosity in allowing us time on their IBM-650 computer.

### APPENDIX A

$k = m_\alpha v_\alpha / \hbar$  where  $m_\alpha$  = reduced mass in channel  $\alpha$  and  $v_\alpha$  = relative velocity in channel  $\alpha$ .

$\eta = z_1 z_2 e^2 / \hbar v_\alpha$ .

$Y_l^m(\theta, \phi)$  = normalized spherical harmonic.

$\chi_s^{m_s}$  = spin wave function.

$\sigma_l = \arg \Gamma(1 + l + i\eta)$ .

$\alpha_l = \sigma_l - \sigma_0 = \sum_{s=1}^l \tan^{-1}(\eta/s)$ .

$\phi_l$  = hard sphere phase shift =  $-\arctan(F_e/G_e)$ .

$\beta^{J^\pi}$  = resonant phase shift.

$l(l')$  = orbital angular momentum of incident (outgoing) particle.

$\Gamma$  = total width (experimental) of the state.

$\Gamma_{\alpha l}$  = partial width in channel  $\alpha$  with orbital angular momentum  $l$ .

$S$  = channel spin in the incident channel.

$S'$  = channel spin in the outgoing channel.